Research Article

Alinda Oyku Akar, Umit Hakan Yildiz, and Umit Tayfun*

Investigations of polyamide nano-composites containing bentonite and organo-modified clays: Mechanical, thermal, structural and processing performances

https://doi.org/10.1515/rams-2021-0025
Received Dec 10, 2019; accepted Jul 24, 2020

Abstract: Polyamide 6 (PA) matrix was reinforced with Na-activated bentonite, amino functional silane treated bentonite and organo-modified clays at different concentrations. The preparation of composites was carried out using melt-blending method and the test samples were prepared by injection-molding process. Mechanical, thermal, structural and processing investigations of PA based composites were reported performing via tensile, hardness, and impact tests, differential scanning calorimetry (DSC), thermal gravimetric analysis (TGA), scanning electron microscopy (SEM), X-ray diffraction analysis (XRD) and force measurements, respectively. According to mechanical test results, additions of fillers to PA matrix caused slight improvements for tensile strength and modulus parameters. Silane treated BNT exhibited improvement in mechanical results compared to Na-activated bentonite additions. Thermal studies revealed that decomposition and melting temperatures of PA shifted to higher values after inclusion of clay into polymer matrix. Results confirmed that organo-clay and bentonite additions with their lower filling ratios yielded enhancements for the mechanical and thermal performance of polyamide.

Keywords: organo-clay; polyamide; nano-composites; bentonite; extrusion

***Corresponding Author: Umit Tayfun:** Inovasens Ltd., Technopark Izmir, 35430 Izmir, Turkey;
Email: umit.tayfun@inovasens.com
Alinda Oyku Akar: Esan, R&D Center, 34852, Istanbul, Turkey; Chemical Eng. Dept., Gebze Technical University, 41400 Kocaeli, Turkey
Umit Hakan Yildiz: Inovasens Ltd., Technopark Izmir, 35430 Izmir, Turkey; Chemistry Dept., Izmir Institute of Technology, 35430 Izmir, Turkey

1 Introduction

Polymer composites are the materials which compose of mainly two different phases. Filler particles are embedded in continuous polymeric matrix. Filler phase generally is responsible of reinforcement for the performance of the material. The final properties of polymer composites depend on the mixing homogeneity and adhesion between phases [1, 2]. Interactions between filler and matrix phases can be formed in molecular dimensions thanks to nano-scale additives have at least one specific length scale of the order of nanometers. Because of this, nanocomposites exhibit extraordinary properties more efficiently compared to traditional composites. Recently, NCs have opened the door very widely for new technologies for all areas of the industry due to the large interfacial area between nano-scale additive and polymer matrix [3–5]. For most polar polymers, alkylammonium surfactants are adequate to achieve intercalated or exfoliated structure and promote the nanocomposite formation [6–8].

Bentonite is natural clay obtained from volcanic deposit areas. Bentonite powder mainly consists of silicate and alumina in its composition. Silicate containing portion includes predominantly smectite minerals such as montmorillonite. Smectite crystallites themselves are three-layer clay minerals. They consist of two tetrahedral layers and one octahedral layer. The silicate layers have a slight negative charge that is compensated by exchangeable ions in the inter-crystallite region. Bentonite mineral is used widely on several areas including paints, medical products, ceramics, papers, cosmetics and packaging [9, 10].

Polyamide (PA) is a semi-crystalline engineering polymer. PA has an amide linkage in the polymer backbone. Aliphatic or semi-aromatic polyamides that are melt-processable are also referred to as nylon. This definition encompasses a wide variety of products, most notably PA 66 and PA6, which represent the vast majority. PA 6 can fulfill the demand of various capabilities for the use of polyamide

based composites in timing belt cover, body panel, air intake manifolds, wiring clips, wheel covers and under-the-hood applications [11–13].

Several research efforts are existing to investigate the basic properties of nanoclay containing PA based nanocomposites in the literature. In these studies, enhancements of thermal stability and mechanical performance were reported [14–17]. According to their findings, researchers reported significant improvements for investigated properties of PA-based nanocomposites as the homogeneous dispersion of nanoclay into PA matrix was achieved.

The novelty of this research work is to represent the distinctive experimental data that postulates the weight saving, ease of processing and functionality performances of PA based nano-composites containing organo-clay and bentonite minerals. These characteristics are highly required in mainly transportation field. This research is primarily focused on the enhancement of basic properties of PA based composites by incorporation of bentonite and organo-modified clays. Incorporation of bentonite and organo-modified clays into PA matrix were performed individually for different concentrations. Additionally, the effects of different modification types were also examined to observe the interactions between the reinforcing agent and matrix through different surface modified grades. Production methods of PA based composites have been chosen as conventional extrusion and injection molding processing techniques due to their ability of cost-effectiveness, practical and compatible adaptation for large scale applications. Investigation of structural, thermal and mechanical performances of unfilled PA and relevant composites were carried out using X-ray diffraction analysis (XRD), differential scanning calorimetry (DSC), thermal gravimetric analysis (TGA), tensile, hardness, and impact tests, respectively. In addition to these findings, density measurements of nano-composites were performed in order to evaluate their weight-reduction ability for transportation applications. Force measurements were conducted during melt-mixing process of composites in order to provide information related to the energy consumption during the application of extrusion process in large scale production of these nano-composites.

2 Experimental Procedure

2.1 Materials

The commercial polyamide 6 (Bergamid B65 W25) was supplied from PolyOne, USA. Dry ground Na-activated bentonite (EBNT SA), amino functional silane treated bentonite (EBNT) and organo-modified clays, NC 130 (EsanNANO 1-130) and NC 140 (EsanNANO 1-140), were obtained from Esan Eczacıbaşı Industrial Raw Materials Co., Istanbul, Turkey. NC 130 and NC 140 clays were obtained as modified by producer using quaternary ammonium salts involving dimethyl and dimethyl benzyl units, respectively.

2.2 Preparation of Composites

PA and additives were pre-dried at 80°C for 2 hours prior to compounding. The preparation of composites was carried out using a lab-scale twin-screw micro-extruder (MC 15 HT, DSM Xplore Instruments) with the loading ratios ranging from 1.0% to 20.0% by weight. Process temperature, screw speed and mixing time were 230°C, 100 rpm and 5 min, respectively. The unfilled PA was also mixed under the same conditions in order to provide clear comparison with its composites. PA and relevant composites were cut into chip form after extrusion process. Test samples were shaped by an injection molding instrument (Micro-injector, Daca Instruments) in which barrel temperature of 235°C and the injection pressure of 5 bar were applied. Injection-molded dog-bone shape specimens with the dimensions of 7.4×2.1×80 mm^3 were obtained from the injection molding process.

2.3 Characterization Methods

Force measurements of samples were performed by DSM Xplore software during extrusion process. The screw force values in the melt were determined by the function of mixing time using rheological software of the micro-compounder. In order to investigate structural properties of samples X-ray diffraction analysis (XRD) was utilized by X'Pert PRO, PAN analytical with Ni-filtered CuKα radiation (λ = 0.154 nm) at 45 kV and 40 mA. JEOL JSM-6400 electron microscope was utilized to visualize the dispersion of BNT and NC particles into PA matrix. Surfaces of fractured samples obtained from impact test were coated with gold to create conductive surfaces. SEM micrographs were taken at x1000 and x4000 magnifications. Density measurements were conducted to composite samples using a digital density meter (Easy D30, Mettler Toledo). All the results represent an average value of three samples for thermal tests (TGA and DSC) and density measurements. The characterizations of the tensile properties were carried out using Lloyd LR 30 K universal tensile testing machine by using load cell of 5 kN at crosshead speed of 5 cm/min

according to the ISO 37 standard. Tensile strength, percentage elongation at break and tensile modulus values were recorded. Impact test was performed according to ASTM D256 standard with 4J pendulum using Coesfeld material impact tester. All the results represent an average value of five samples with standard deviations. Shore hardness of composites was evaluated by TQC Sheen BV hardness tester according to ISO 868 standard. Thermal behaviors of samples were determined using Netzsch Jupiter STA 449 F3. TGA and DSC measurements were carried out in the temperature range of 25°C to 600°C with a heating rate of 10°C/min under nitrogen flow of 50 ml/min.

3 Results and discussion

3.1 Structural analysis

Structural properties of BNT and NC in their bulk form and into PA matrix were studied by XRD analysis. Test results of bulk and composite samples are represented in Figure 1a and Figure 1b, respectively. The distinct band located at nearly $2\theta = 6^\circ$ as can be seen for NC samples in Figure 1a. The disappearance of these characteristic bands completely for PA/NC 130 1 and PA/NC 140 1 corresponds to intercalated structure of clay layers into PA matrix [18]. The characteristic Bragg peaks of nanoclay-filled composites at nearly $2\theta = 10^\circ$ (Figure 1b) show increase in d-spacing values associated with the enhancement dispersion with the help of quaternary ammonium salts. NC 130 and silane-modified BNT exhibit peaks at higher values confirming enlargement of interlayer spacing of the mineral. Inclusions of NC 140 with 1% and NC 130 with 3% amounts cause intercalation and exfoliation structures in PA matrix.

The representative SEM micrographs of composites are displayed in Figure 2. Si-BNT particles show slightly higher dispersion homogeneity than BNT particles according to their SEM images. Agglomerations are observed for NC 130 and NC 140 containing composites at their highest loading ratio (20%) as indicated by circles in SEM micrographs. On the other hand, large aggregates disappear for 1% concentration of NC loaded composites which arises from the more homogeneous dispersion of clay layers into PA phase at low adding amount. SEM images of composites provide visual evidence for previously discussed XRD finding based on the separation of the clay layers in PA matrix.

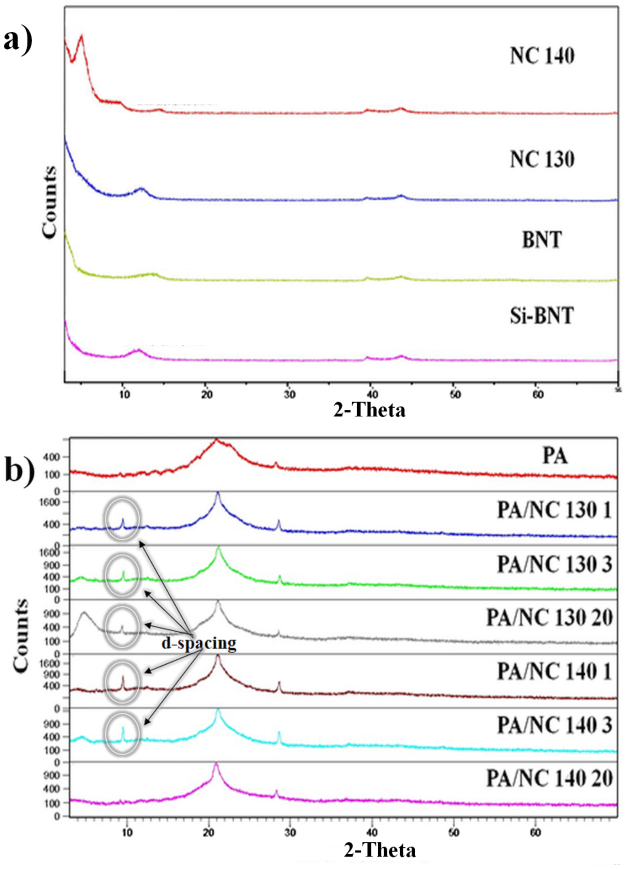

Figure 1: XRD results of bulk and composite samples.

3.2 Force measurements

Shear force values are important parameters in order to determine the production cost during processing of the polymeric materials in industrial applications where melt blending is the preferred production method. According to force values recorded during extrusion process of materials (Figure 3), bentonite additions caused increase for shear force of unfilled PA. The final shear force values of composites are improved by increase in loading ratio of bentonite. Silane modified BNT exhibits reduction for shear force by behaving like a plasticizer. NC inclusions with the highest concentration (20%) cause level up for exerted force due to the formation of agglomerates. According to these results, increase in concentration of BNT and NC led to obtain higher amount of exerted force stem from the formation of elevated shear rates during extrusion by the addition of higher levels of additives [19, 20].

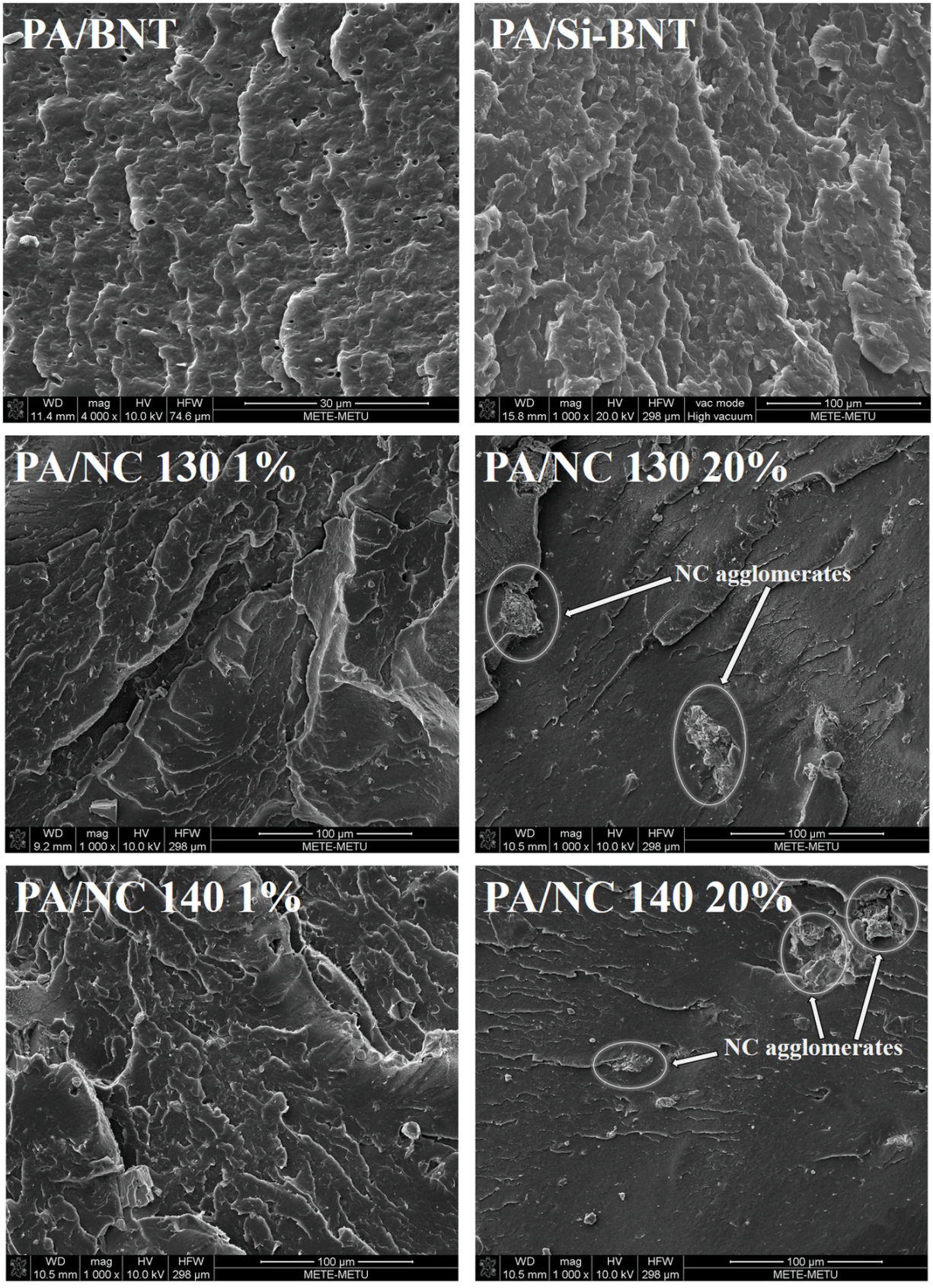

Figure 2: SEM micrographs of composites.

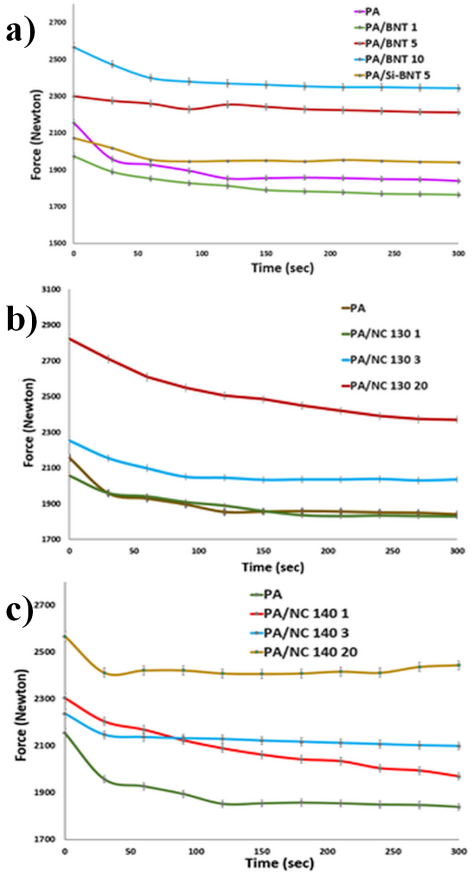

Figure 3: Force values of PA and composites.

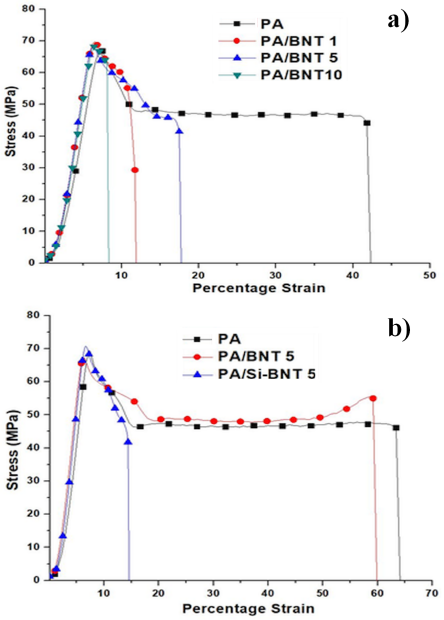

Figure 4: Stress–strain curves of BNT-filled composites.

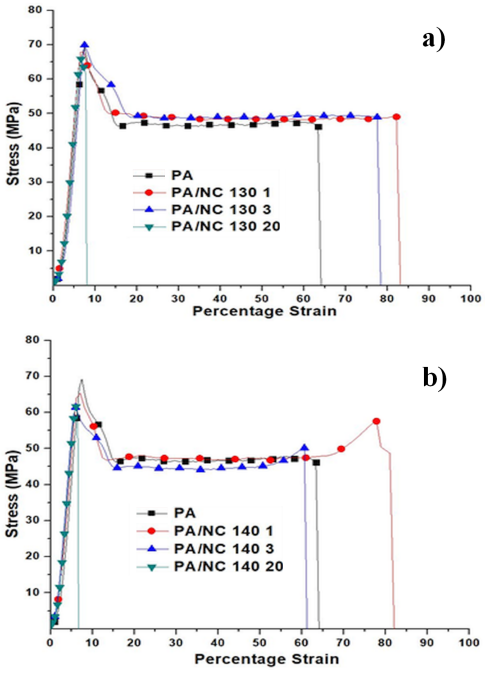

Figure 5: Stress–strain curves of NC-filled composites.

3.3 Tensile properties

The tensile test characteristics of composites are investigated by the stress–strain curves shown in Figure 4 for PA/BNT, Figure 5 for PA/NC composites and the relevant test data are listed in Table 1. It can be seen that BNT additions yield slight improvement for tensile strength values of unfilled PA. The greatest increase in tensile strength is observed for Si-BNT loaded composite thanks to enhanced surface interaction between PA and silane modified BNT. These strong chemical interactions stem from the amino group of silane coupling agent which promotes the elevation for tensile strength of composite [21, 22].

All of the BNT-filled composites give higher tensile modulus values than that of PA. Elongation of PA also increases with the incorporation of BNT at 5% concentration. NC additions at low filling ratios exhibit increasing trend for tensile strength of unfilled PA. Reduction of tensile strength after 3% loading level of NC is attributed to stress concentrator action of organoclay agglomerates [23].

Tensile modulus of PA is not affected by NC inclusions. However, BNT additions caused slight increase in modulus of unfilled PA. These results are agreement with the theoretical predictions of tensile modulus in literature [24–26]. NC containing composites give increase drastically for elongation values at their lower amounts. These findings imply that layered structure of NC causes plasticizing effect for PA matrix [27, 28].

Table 1: Mechanical test results of PA and its composites.

Samples	Tensile Strength (MPa)	Tensile Modulus (GPa)	Elongation (%)	Hardness (Shore)
PA	67.0(1.1	1.6(0.1	12.0(0.7	64.2±0.1
PA/BNT 1	69.4(1.4	1.7(0.1	8.2(0.5	67.1±0.1
PA/BNT 5	68.2(1.6	1.7(0.1	17.6(0.9	73.4±0.1
PA/Si-BNT 5	70.8(1.3	1.7(0.1	14.5(0.7	66.8±0.1
PA/BNT 10	68.4(1.6	1.7(0.2	9.1(0.3	72.5±0.1
PA/NC 130 1	68.5(1.7	1.6(0.1	82.7(1.1	65.2±0.1
PA/NC 130 3	69.0(1.4	1.6(0.2	78.3(0.7	65.7±0.1
PA/NC 130 20	65.9(1.8	1.7(0.1	8.2(0.2	75.3±0.1
PA/NC 140 1	68.1(1.3	1.6(0.2	81.3(0.9	65.0±0.1
PA/NC 140 3	61.7(1.9	1.6(0.2	61.2(0.8	65.6±0.1
PA/NC 140 20	61.4(1.6	1.6(0.1	6.4(0.4	74.9±0.1

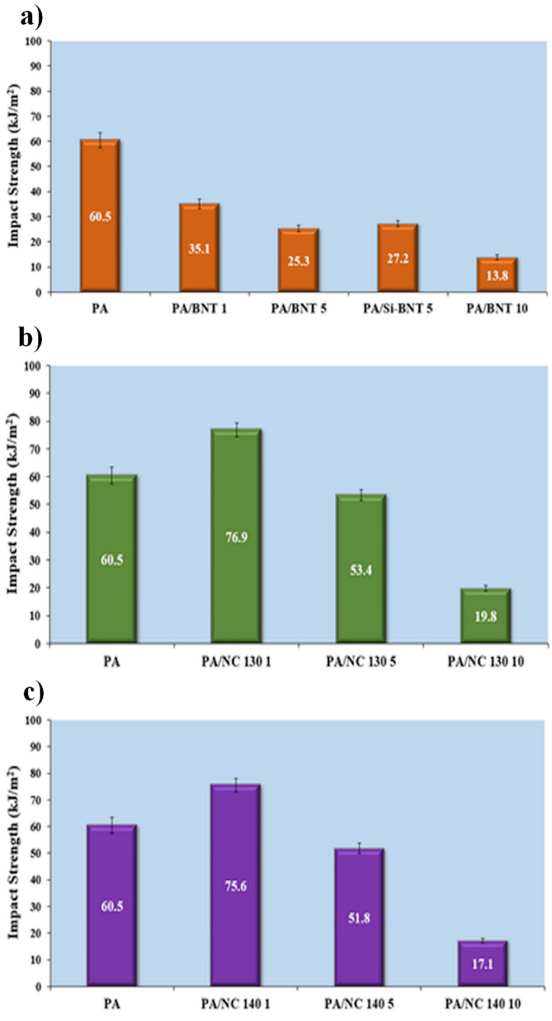

Figure 6: Impact energy values of PA and composites.

3.4 Hardness test

Shore hardness is a characteristic parameter for polymeric materials. The Shore D hardness values of PA and its composites are listed in the last column of Table 1. It can be seen from these values that NC and BNT additions lead to significant increase in Shore D hardness of PA. The highest loading levels of additives display around 10 points higher hardness values than that of unfilled PA. Silane treated BNT addition causes reduction for hardness compared to untreated BNT. Similar results are observed from literature that BNT addition yields higher Shore hardness values compared to neat polymer [29, 30].

3.5 Impact resistance

The impact energy values of composites are demonstrated in Figure 6. Impact energy value of PA exhibits reduction trend with BNT additions. Impact energy decreases with the increase in loading level of BNT. This trend may be described by the formation of stress failures between BNT and PA matrix. BNT particles cause restriction for deformation ability of PA phase which results in decrease for the total free energy of the composite system. Silane modified BNT yield slightly higher impact energy with respect to unmodified BNT thanks to formation of strong interaction between amino functional group of silane layer and PA phase [31]. Impact energy of PA is enhanced about 15 points higher level with the addition of the lowest filling ratios for NC 130 and NC 140. NC 140 loaded PA gives slightly higher impact energies compared to NC 130. PA gains toughness which means ability to absorb more energy during deformation after incorporation with 1% of NC 130 and 1% of NC 140 thanks to homogeneous dispersion of clay layers.

3.6 Density measurements

In addition to a high level of mechanical performance, lightweight composite parts are highly required by automotive manufacturers. Nanocomposites exhibit resistance to impact and tensile deformations as mentioned earlier discussions besides providing weight saving behavior in transporting applications. Density values of PA and composites are listed in Table 2. According to these results, BNT leads to an increase in density values of composites since it has a higher density relative to PA. NC containing composites display reduction trend for densities compared to unfilled PA. The inclusion of NC 130 at its lowest concentration gives the best weight reduction value which may be important for automotive applications. However, effective density of composites depends on the dispersion homogeneity of BNT and NC. The presence of agglomerated filler particles in measured part of samples may lead to obtaining higher bulk density values compared to the effective density of homogeneously dispersed composite system [32]. Accordingly, sharp improvement in density values of 20% NC loaded composites corresponds to formation of large agglomerates of nanoclay in PA phase as confirmed by SEM images of these candidates (Figure 2).

Table 2: Density values of PA and composites.

Samples	Density (g/cm^3)
PA	1.150
PA/BNT 1	1.151
PA/BNT 5	1.153
PA/Si-BNT 5	1.147
PA/BNT 10	1.154
PA/NC 130 1	1.125
PA/NC 130 3	1.131
PA/NC 130 20	1.172
PA/NC 140 1	1.117
PA/NC 140 3	1.112
PA/NC 140 20	1.147

3.7 Thermal properties

DSC curves of PA/BNT, PA/NC 130 and PA/140 composites are given in Figure 7a, Figure 7b and Figure 7c, respectively. DSC data including melting temperature (T_m) of PA and composites are indicated in Table 3. BNT additions cause shifting of T_m value for unfilled PA to nearly two-point higher temperatures. However, silane-modified BNT gives

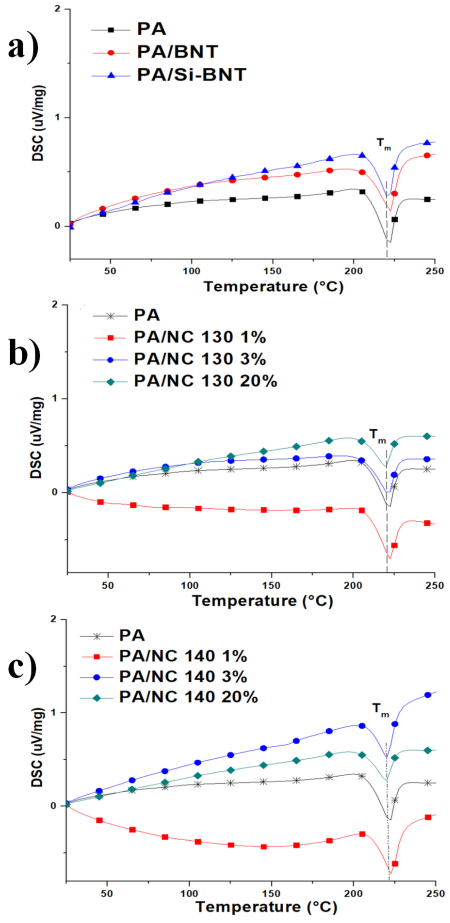

Figure 7: DSC curves of PA and composites.

slightly lower Tm compared to neat BNT. NC inclusions also lead T_m of unfilled PA to higher temperatures. The highest T_m is obtained for nano-composites reinforced with the lowest NC concentration since the segmental motion of the PA chains may be prevented by the intercalated or exfoliated clay layers at their lower loading levels [33]. NC incorporated samples for their low concentrations display relatively higher T_m values. However, melting temperature of nano-composites containing 20%wt of NC 130 and NC 140 exhibit nearly identical T_m with that of unfilled PA. The intensity and area of the endothermic peak indicate the enthalpy of melting which is attributed to the melting of PA crystals [34, 35].

According to Figure 7, 1%wt of NC additions display slight increase or no change for the melting enthalpy of unfilled PA. On the other hand, reduced intensity and area were observed for 20%wt of NC filled composites with respect to PA. This result is related to the nucleation effect of NC at their lower concentrations due to the formation of intercalated clay layers into PA structure [36].

Table 3: TGA and DSC data of PA and composites.

Samples	T_m (°C)	T_d (°C)	Char (%)
PA	220.1	420.8	1.19
PA/BNT 1	221.7	420.9	3.51
PA/BNT 5	222.5	421.2	7.46
PA/Si-BNT 5	221.2	424.9	7.69
PA/NC130 1	222.9	426.1	1.64
PA/NC130 3	221.5	420.1	3.51
PA/NC130 20	219.7	416.2	10.74
PA/NC140 1	223.0	424.6	1.82
PA/NC140 3	221.3	417.4	3.88
PA/NC140 20	220.8	415.8	11.18

TGA curves of PA/BNT, PA/NC 130 and PA/140 composites are presented in Figure 8. TGA data including decomposition temperature (T_d) and char content of samples are provided in Table 3. According to TGA curves, the weight loss of unfilled PA occurs in a single step degradation. T_d values indicate the temperatures which maximum weight loss rate occur. Enhancement of thermal stability is highly required for high temperature durability of polymer-based composites in numerous applications. Improvement of thermal stability is confirmed by shifting of T_d values to higher levels. TGA results show that, thermal stability of PA is enhanced with Si-BNT inclusions which lead to slow down for degradation rate compared to untreated BNT. Organoclay additions cause remarkable increase for T_d at their lowest filling ratio (1%wt). The highest loading level of NC exhibits reduction for T_d regardless of organo-clay type due to disappearance of exfoliated clay layers. The char yield of unfilled PA also increases by the amount of incorporated additives increase. Similar trends are obtained in the literature related to BNT and nanoclay loaded polymer matrices [37–39].

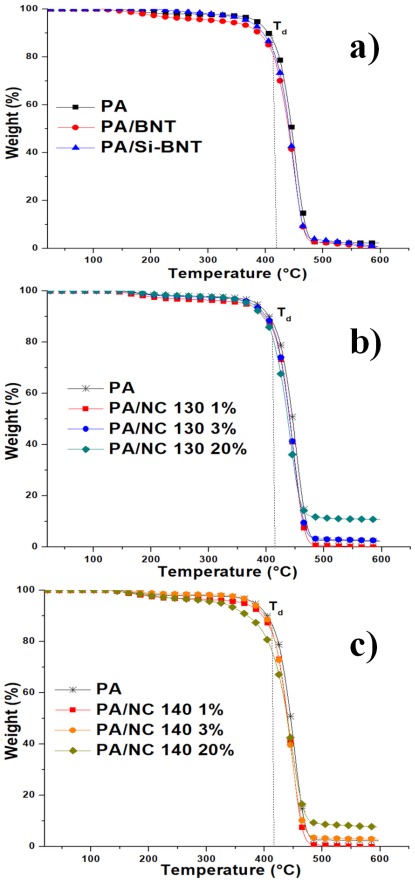

Figure 8: TGA curves of PA and composites.

4 Conclusion

In this current study, the effect of bentonite and organoclay additions on the mechanical, structural, thermal and physical properties of PA 6 based composites were reported. BNT and NC inclusions at their lower amounts cause increase in mechanical strength of PA. Further additions of NC and BNT exhibit significant reductions. Silane modified BNT yields higher tensile strength compared to the unmodified one thanks to enhancement of interfacial interactions between BNT and PA phases. Elongation of PA increases more than 6 times by inclusion of 1% content for both types NC. Shore hardness of PA is improved with BNT and NC inclusions. According to XRD and SEM investigations, agglomerations are observed for higher concentrations of NC, whereas intercalation/exfoliation structures in PA matrix are achieved for lower loading levels of NC. Both BNT and NC additions at 1%wt concentration are resulted in shifting of melting temperature of unfilled PA to higher values. TGA results revealed that thermal stability of PA is improved with BNT incorporations. The inclusion of additives with higher filling ratios leads to an increase in shear force, however, silane modifications help to reduce the force, thus resulting in less power and electricity usage in large scale applications. Incorporation of NC to PA gives much higher impact resistance than BNT, especially for lower concentrations. Nano-composites containing 1% of NC display the best mechanical and thermal performance besides reduction of weight which provides significant output in the case of manufacture of automotive parts.

Acknowledgement: This research study was represented in International Conference on Materials and Nanomaterials MNs-19 which was held on 17-19 July 2019 at Paris, France.

Funding information: Authors state no funding involved.

Data availability statement: The data that support the findings of this study are available from the corresponding author, upon reasonable request.

Conflict of interest: The authors declare that they have no known competing financial interests or personal relationships that could have appeared to influence the work reported in this paper.

References

[1] Bafekrpour, E. *Advanced Composite Materials: Properties and Applications*. De Gruyter, Berlin, 2017. DOI: https://doi.org/10.1515/9783110574432.

[2] Donnet, J. B. Nano and microcomposites of polymers elastomers and their reinforcement. *Composites Science and Technology*, Vol. 63, No. 8, 2013, pp. 1085–1088.

[3] Ray, S. S., and M. Okamoto. Polymer/layered silicate nanocomposites: A review from preparation to processing. *Progress in Polymer Science*, Vol. 28, No. 11, 2003, pp. 1539–1641.

[4] Albdiry, M., B. Yousif, H. Ku, and K. Lau. A critical review on the manufacturing processes in relation to the properties of nanoclay/polymer composites. *Journal of Composite Materials*, Vol. 47, No. 9, 2013, pp. 1093–1115.

[5] Zanetti, M., S. Lomakin, and G. Camino. Polymer layered silicate nanocomposites. *Macromolecular Materials and Engineering*, Vol. 279, No. 1, 2000, pp. 1–9.

[6] Gelfer, M. Y., H. H. Song, L. Liu, B. S. Hsiao, B. Chu, M. Rafailovich, M. Si, and V. Zaitsev. Effects of organoclays on morphology and thermal and rheological properties of polystyrene and poly(methyl methacrylate) blends. *Journal of Polymer Science. Part B, Polymer Physics*, Vol. 41, No. 1, 2003, pp. 44–54.

[7] Seyidoglu, T., and U. Yilmazer. Modification and characterization of bentonite with quaternary ammonium and phosphonium salts and its use in polypropylene nanocomposites. *J. Thermoplast. Compos. Mater.*, Vol. 28, No. 1, 2015, pp. 86–110.

[8] Chaiko, D. J. Activation of organoclays and preparation of polyethylene nanocomposites. e-Polymers, 2006, 6, 1618–7229.

[9] Klein, C. and C. S. Hurlbut. *Manual of Mineralogy*, 21st ed. Wiley, 1998.

[10] Clem, A. G., and R. W. Doehler. *Industial Apllications of Bentonite*. Macmillan, New York, 1963.

[11] Mallick, P. K. Advanced materials for automotive applications: An overview. In *Advanced materials in automotive engineering*, Woodhead Publishing, 2012. DOI: https://doi.org/10.1533/9780857095466.5.

[12] Gendre, L., J. Njuguna, H. Abhyankar, and V. Ermini. Mechanical and impact performance of three-phase polyamide 6 nanocomposites. *Materials & Design*, Vol. 66, 2015, pp. 486–491.

[13] Varley, R. J., A. M. Groth, and K. H. Leong. Polyamide blend-based nanocomposites. *Polymer International*, Vol. 57, 2008, pp. 618–625.

[14] Zhang, C. Progress in semicrystalline heat-resistant polyamides. e-Polymers. Vol. 18, 2018, pp. 373–408.

[15] Fornes, T. D., D. L. Hunter, and D. R. Paul. Nylon-6 nanocomposites from alkyl ammonium-modified clay: The role of alkyl tails on exfoliation. *Macromolecules*, Vol. 37, No. 5, 2004, pp. 1793–1798.

[16] Ryba, J., A. Ujhelyiová, M. Krištofič, and I. Vassová. Thermal properties of PA 6 and PA 6 modified with copolyamides and layered silicates. *Journal of Thermal Analysis and Calorimetry*, Vol. 101, No. 3, 2010, pp. 1027–1037.

[17] Scaffaro, R., L. Botta, A. Frache, and F. Bellucci. Thermo-oxidative ageing of an organo-modified clay and effects on the properties of PA6 based nanocomposites. *Thermochimica Acta*, Vol. 552, 2013, pp. 37–45.

[18] Akar, A. O. and J. Hacaloglu. Preparation and characterization of poly (lactic acid) composites involving aromatic diboronic acid and organically modified montmorillonite. *Journal of Thermal Analysis and Calorimetry*, 2020. Vol. 143, 2021, pp. 3117–3126.

[19] Delay, J. M. and K. F. Wissbrun. *Melt rheology and its role in plastics processing: Theory and applications*. Van Nostrand Reinhold, New York, 1990.

[20] Chung, C. I. *Extrusion of polymers: Theory & practice*. Carl Hanser Verlag GmbH, Munich, 2019. DOI: https://doi.org/10.3139/9781569907382.

[21] Salem, T. F., S. Tirkes, A. O. Akar, and U. Tayfun. Enhancement of mechanical, thermal and water uptake performance of TPU/jute fiber green composites via chemical treatments on fiber surface. e-Polymers, Vol. 20, No. 1, 2020, pp. 133–143.

[22] Yang, R., Y. Liu, K. Wang, and J. Yu. Characterization of surface interaction of inorganic fillers with silane coupling agents. *Journal of Analytical and Applied Pyrolysis*, Vol. 70, No. 2, 2003, pp. 413–425.

[23] Tayfun, U. and M. Dogan. Improving the dyeability of poly (lactic acid) fiber using organoclay during melt spinning. *Polymer Bulletin*, Vol. 73, No. 6, 2016, pp. 1581–1593.

[24] Shahriari-Kahkeshi M. and M. Moghri. Prediction of tensile modulus of PA-6 nanocomposites using adaptive neuro-fuzzy inference system learned by the shuffled frog leaping algorithm. e-Polymers. 2017, Vol. 17, 187–198.

[25] Moghri, M., H. Shamaee, H. Shahrajabian, and A. Ghannadzadeh. The effect of different parameters on mechanical properties of PA-6/clay nanocomposite through genetic algorithm and response surface methods. *International Nano Letters*, Vol. 5, No. 3, 2015, pp. 133–140.

[26] Moghri, M., S. I. S. Shahabadi, and M. Madic. Modeling tensile modulus of (polyamide 6)/nanoclay composites: Response surface method vs. taguchi-optimized artificial neural network. *J. Vinyl Addit. Technol.*, Vol. 22, No. 1, 2016, pp. 29–36.

[27] Liborio, P., V. A. Oliveira, and M. F. V. Marques. New chemical treatment of bentonite for the preparation of polypropylene nanocomposites by melt intercalation. *Applied Clay Science*, Vol. 111, 2015, pp. 44–49.

[28] Mészáros, L. Elastic recovery of polyamide 6 matrix nanocomposites and their basalt fiber co-reinforced hybrids. e-Polymers, Vol. 17, 2017, pp. 349–354.

[29] Alhallak, L. M., S. Tirkes, and U. Tayfun. Mechanical, thermal, melt-flow and morphological characterizations of bentonite-filled ABS copolymer. Rapid Prototyping Journal, Vol. 26, No. 7, 2020, pp. 1305–1312.

[30] Fu, S. Y., X. Q. Feng, B. Lauke, and Y. W. Mai. Effects of particle size, particle/matrix interface adhesion and particle loading on mechanical properties of particulate–polymer composites. *Com-*

posites. Part B, Engineering, Vol. 39, No. 6, 2008, pp. 933–961.
[31] Yang, R., Y. Liu, K. Wang, and J. Yu. Characterization of surface interaction of inorganic fillers with silane coupling agents. *Journal of Analytical and Applied Pyrolysis*, Vol. 70, No. 2, 2003, pp. 413–425.
[32] Chen, B. and J. R. Evans. Nominal and effective volume fractions in polymer-clay nanocomposites. *Macromol.*, Vol. 39, No. 5, 2006, pp. 1790–1796.
[33] Dogan, M. and E. Bayramli. The flame retardant effect of aluminum phosphinate in combination with zinc borate, borophosphate, and nanoclay in polyamide-6. *Fire and Materials*, Vol. 38, No. 1, 2014, pp. 92–99.
[34] Schick, C. Differential scanning calorimetry (DSC) of semicrystalline polymers. *Analytical and Bioanalytical Chemistry*, Vol. 395, No. 6, Nov. 2009, pp. 1589–1611.
[35] Khanna, Y. P., W. P. Kuhn, and W. J. Sichina. Reliable measurements of the nylon 6 glass transition made possible by the new dynamic DSC. *Macromolecules*, Vol. 28, No. 8, 1995, pp. 2644–2646.
[36] Fornes, T. D. and D. R. Paul. Structure and properties of nanocomposites based on nylon-11 and-12 compared with those based on nylon-6. *Macromolecules*, Vol. 37, No. 20, 2004, pp. 7698–7709.
[37] Jang, B. N. and C. A. Wilkie. The effect of clay on the thermal degradation of polyamide 6 in polyamide 6/clay nanocomposites. *Polymer*, Vol. 46, No. 10, 2005, pp. 3264–3274.
[38] Elkawash, H., S. Tirkes, F. Hacioglu, and U. Tayfun. Physical and mechanical performance of bentonite and barite loaded low density polyethylene composites: Influence of surface silanization of minerals. *Journal of Composite Materials*, Vol. 54, No. 28, 2020, pp. 4359–4368.
[39] Gilman, J. W. Flammability and thermal stability studies of polymer layered-silicate (clay) nanocomposites. *Applied Clay Science*, Vol. 15, No. 1-2, 1999, pp. 31–49.